

# UC San Diego

## UC San Diego Previously Published Works

### Title

Topcolor in the LHC Era

### Permalink

<https://escholarship.org/uc/item/6tj5w28t>

### Authors

Simmons, EH  
Chivukula, RS  
Coleppa, B  
[et al.](#)

### Publication Date

2013-05-01

### DOI

10.1142/9789814412322\_0023

Peer reviewed

## TOPCOLOR IN THE LHC ERA\*

E.H. SIMMONS<sup>†</sup> and R.S. CHIVUKULA

*Department of Physics and Astronomy, Michigan State University,  
East Lansing, MI 48824, USA*

*\* E-mail: esimmons@msu.edu, sekhar@msu.edu*

B. COLEPPA and H.E. LOGAN

*Ottawa-Carleton Institute for Physics, Carleton University,  
Ottawa, Ontario K1S 5B6, Canada*

*E-mail: barath@physics.carleton.ca, logan@physics.carleton.ca*

A. MARTIN

*Theoretical Physics Department, Fermilab,  
Batavia, IL 60510, USA*

*E-mail: aomartin@fnal.gov*

Ongoing LHC searches for the standard model Higgs Boson in  $WW$  or  $ZZ$  decay modes strongly constrain the top-Higgs state predicted in many models with new dynamics that preferentially affects top quarks. Such a state couples strongly to top-quarks, and is therefore produced through gluon fusion at a rate that can be greatly enhanced relative to the rate for the standard model Higgs boson. As we discuss in this talk, a top-Higgs state with mass less than 300 GeV is excluded at 95% CL if the associated top-pion has a mass of 150 GeV, and the constraint is even stronger if the mass of the top-pion state exceeds the top-quark mass or if the top-pion decay constant is a substantial fraction of the weak scale. These results have significant implications for theories with strong top dynamics, such as topcolor-assisted technicolor, top-seesaw models, and certain Higgsless models.

*Keywords:* topcolor, composite Higgs bosons, collider phenomenology.

### 1. Introduction

The Large Hadron Collider seeks to uncover the agent of electroweak symmetry breaking and thereby discover the origin of the masses of the elemen-

---

\*This talk from KMIIN 2011 reports on work first published by the authors as Ref. 1.

<sup>†</sup>The presenter of this work at KMIIN.

tary particles. In the standard model,<sup>2</sup> electroweak symmetry breaking occurs through the vacuum expectation value of a fundamental weak-doublet scalar boson. Via the Higgs mechanism,<sup>3</sup> three of the scalar degrees of freedom of this particle become the longitudinal states of the electroweak  $W^\pm$  and  $Z$  bosons and the last, the standard model Higgs boson ( $H_{SM}$ ), remains in the spectrum. Recently, both the ATLAS<sup>4</sup> and CMS<sup>5</sup> collaborations have set limits on the existence of a standard model Higgs boson. In this talk we show what these limits imply about the “top-Higgs” ( $H_t$ ) expected in topcolor assisted technicolor models and other models with new strong dynamics preferentially affecting the top quark.

Topcolor assisted technicolor (TC2)<sup>6–9</sup> is a dynamical theory of electroweak symmetry breaking that combines the ingredients of technicolor<sup>10,11</sup> and top condensation.<sup>12–16</sup> Top condensation and the top quark mass arise predominantly from “topcolor”,<sup>17</sup> a new QCD-like interaction that couples strongly to the third generation of quarks.<sup>a</sup> Technicolor then provides the bulk of electroweak symmetry breaking via the vacuum expectation value of a technifermion bilinear. LHC constraints on technicolor itself are discussed in the KMIIN talk “Technicolor in the LHC Era” given by R.S. Chivukula, which is also reported in these proceedings.

TC2 is an important potential ingredient in theories of dynamical electroweak symmetry breaking.<sup>19</sup> In particular, it is difficult to construct technicolor theories which accommodate the heavy top-quark without also producing large and experimentally forbidden corrections to the ratio of  $W$ - and  $Z$ -boson masses<sup>20</sup> or to the coupling of the  $Z$ -boson to bottom-quarks.<sup>21</sup> By separating the sector responsible for top-quark mass generation from that responsible for the bulk of electroweak symmetry breaking, TC2 alleviates these difficulties. We have previously introduced a consistent low-energy effective theory for models with separate sectors for generating the top mass and the vector boson masses, known as the “top-triangle moose” model.<sup>22</sup> This theory, which combines Higgsless and topcolor models, can be used to investigate the phenomenology of TC2 theories<sup>23</sup> and other theories with strong top dynamics, and we employ it in that capacity in this talk.

As we shall soon review, theories with strong top dynamics generically include a top-Higgs state – a state with the same quantum numbers as

---

<sup>a</sup>Additional interactions are also included to prevent formation of a  $b$ -quark condensate and, hence, allow for a relatively light  $b$ -quark; the simplest example<sup>6</sup> is an extra  $U(1)$  interaction, giving rise to a topcolor  $Z'$ ; other ideas are discussed in Ref. 18.

the standard model Higgs boson, a mass of generally less than 350 GeV, and a stronger coupling to top-quarks than the standard model Higgs has. This talk will show that the ATLAS<sup>4</sup> and CMS<sup>5</sup> searches for the standard model Higgs exclude, at 95% CL, a top-Higgs with a mass less than 300 GeV provided that the associated top-pion states have a mass of at least 150 GeV; even heavier top-Higgses are also excluded by the data under certain conditions. These results constrain model-building in theories with strong top dynamics.

## 2. Top-Color Assisted Technicolor: The Scalar Sector

At low energies, any top-condensate model includes the composite weak-doublet scalar boson with the same quantum numbers as the fundamental scalar in the standard model.<sup>24</sup> The vacuum expectation value of the composite weak-doublet scalar boson,  $f_t$ , combined with the technipion decay-constant of the technicolor theory,  $F$ , yield the usual electroweak scale

$$v^2 = \frac{1}{\sqrt{2}G_F} = f_t^2 + F^2 \approx (246 \text{ GeV})^2, \quad (1)$$

where  $G_F$  is the weak-interaction Fermi constant. Motivated by this relation, we define an angle  $\omega$  such that  $f_t \equiv v \sin \omega$ . The factor  $\sin \omega$  indicates the fraction of electroweak symmetry breaking provided by the top condensate. Three of the degrees of freedom of the composite scalar mix with the states in the technicolor spectrum which are the analogs of the pions of QCD. Through the Higgs mechanism,<sup>3</sup> one set of linear combinations become the longitudinal states of the  $W^\pm$  and  $Z$ . The orthogonal combinations, which we denote  $\Pi_t^\pm$  and  $\Pi_t^0$ , remain in the spectrum and are referred to as “top-pions.” Ignoring (small) electromagnetic corrections to their masses, the charged and neutral top-pions are degenerate. The fourth degree of freedom in the composite scalar<sup>b</sup>, which we denote  $H_t$ , is the neutral “top-Higgs.” The phenomenology of the scalar sector of top-condensate models is determined by the masses of the top-Higgs and top-pions,  $M_{H_t}$  and  $M_{\Pi_t}$ , and the value of  $\sin \omega$ . Let us now consider the range of allowed masses and mixing angles, to set the stage for discussing the corresponding scalar phenomenology.

Quantitative analyses of the strong topcolor dynamics<sup>12–16</sup> use the Nambu–Jona-Lasinio<sup>25</sup> (NJL) approximation to the topcolor interactions,

<sup>b</sup>In principle, this degree of freedom will also mix with a state in the technicolor spectrum, a state analogous to the putative “sigma” particle in QCD. In practice such a state has a mass of order a TeV or higher, and this mixing is negligible.

solved in the large- $N$  limit.<sup>26</sup> In this limit, we find the Pagels-Stokar relation<sup>27</sup> for  $f_t$

$$f_t^2 = \frac{N_c}{8\pi^2} m_{t,dyn}^2 \ln \left( \frac{\Lambda^2}{m_{t,dyn}^2} \right), \quad (2)$$

where  $\Lambda$  is the cutoff of the effective NJL theory, which is expected to be of order a few to tens of TeV,<sup>9</sup> and  $m_{t,dyn}$  denotes the portion of the top-quark mass arising from topcolor. The portion of the top-quark mass arising from technicolor interactions (more properly, extended technicolor<sup>28,29</sup> interactions) is expected to be less than or of order the bottom-quark mass, and hence  $m_{t,dyn} \approx m_t$ .<sup>6,19</sup> Varying  $\Lambda$  between 1 and 20 TeV, we find

$$0.25 \lesssim \sin \omega \lesssim 0.5. \quad (3)$$

In the large- $N$ /NJL approximation, we find  $m_{H_t} = 2m_{t,dyn} \approx 350$  GeV. This relation can be modified via QCD interactions which, in the leading-log approximation (here  $\log(\Lambda/M_{H_t})$ ) tend to lower the top-Higgs mass.<sup>16,30</sup> In addition, there can be additional (non leading-log) corrections coming from interactions in the topcolor theory that are not included in the NJL approximation, and also corrections that are subleading in  $N$ . Therefore, while top-Higgs masses less than or of order 350 GeV are expected in these theories, we will discuss results for masses between 200 and 600 GeV.

The top-Higgs couples to top-quarks and to pairs of electroweak bosons, and it does so in a characteristic manner. Since topcolor interactions give rise to  $m_{t,dyn}$ , the bulk of the top mass, and since the expectation value of the composite weak scalar doublet is  $f_t = v \sin \omega$ , the Yukawa coupling of  $H_t$  to top-quarks is

$$y_{H_t} = \frac{\sqrt{2}m_{t,dyn}}{f_t} \approx \frac{y_t}{\sin \omega}, \quad (4)$$

where  $y_t = \sqrt{2}m_t/v$  is the standard model top-quark Yukawa coupling. Hence, the top-Higgs couples more strongly to top-quarks than does the standard model Higgs boson. This enhanced coupling implies an enhancement for top-Higgs production via gluon fusion, relative to the analogous process for the standard model Higgs boson,<sup>31</sup>

$$\frac{\sigma_{gg}(pp \rightarrow H_t)}{\sigma_{gg}(pp \rightarrow H_{SM})} = \frac{\Gamma(H_t \rightarrow gg)}{\Gamma(H_{SM} \rightarrow gg)} \approx \frac{1}{\sin^2 \omega}. \quad (5)$$

In contrast, since the bulk of electroweak symmetry breaking is provided by technicolor (see Eq. (1)), the coupling of the top-Higgs to vector boson

pairs is suppressed relative to the standard model

$$g_{H_t WW/ZZ} = \sin \omega \cdot g_{H_{SM} WW/ZZ} . \quad (6)$$

Hence the top-Higgs vector-boson fusion (VBF) production cross section, and the partial width of  $H_t$  to vector boson pairs, are also suppressed

$$\frac{\sigma_{VBF}(pp \rightarrow H_t)}{\sigma_{VBF}(pp \rightarrow H_{SM})} = \frac{\Gamma(H_t \rightarrow W^+W^-/ZZ)}{\Gamma(H_{SM} \rightarrow W^+W^-/ZZ)} \approx \sin^2 \omega . \quad (7)$$

Since the dominant top-Higgs production pathway is enhanced (see Eq. (5)), the suppression of the vector boson fusion pathway is not of concern.

The crucial issue for the LHC phenomenology of the top-Higgs is the branching ratio  $BR(H_t \rightarrow WW/ZZ)$ : if this branching ratio is sufficiently large, the ATLAS<sup>4</sup> and CMS<sup>5</sup> detectors will be sensitive to the existence of a top-Higgs. As we will now discuss, the branching ratio of the top-Higgs to vector bosons, in turn, depends on the mass of the top-pion. Unlike the top-Higgs mass, the top-pion masses depend on the amount of top-quark mass arising from the (extended) technicolor sector, and on the effects of electroweak gauge interactions.<sup>6,19</sup> These masses are therefore more model-dependent. Since top-pions are in the electroweak symmetry breaking sector, we expect them to be lighter than a TeV.

But top-pions cannot be *too* light. If the charged top-pion  $\Pi_t^+$  were lighter than the top quark, it could appear in top decays,  $t \rightarrow \Pi_t^+ b$ . The Tevatron experiments have searched for this process in the context of two-Higgs-doublet models and set upper bounds of about 10–20% on the branching fraction of  $t \rightarrow H^+ b$ , with  $H^+$  decaying to  $\tau\nu$  or  $c\bar{s}$  (actually, two jets),<sup>32,33</sup> as the top-pion would also do. The branching ratio is<sup>23 c</sup>

$$\begin{aligned} BR(t \rightarrow \Pi_t^+ b) &\approx \frac{\Gamma^{TC2}(t \rightarrow \Pi_t^+ b)}{\Gamma^{SM}(t \rightarrow W^+ b) + \Gamma^{TC2}(t \rightarrow \Pi_t^+ b)} \\ &= \frac{\cot^2 \omega \left(1 - \frac{M_{\Pi_t}^2}{m_t^2}\right)^2}{\left(1 + \frac{2M_W^2}{m_t^2}\right) \left(1 - \frac{M_W^2}{m_t^2}\right)^2 + \cot^2 \omega \left(1 - \frac{M_{\Pi_t}^2}{m_t^2}\right)^2} , \end{aligned} \quad (8)$$

<sup>c</sup>These expressions were derived in the “top-triangle moose” model,<sup>22,23</sup> a low-energy effective theory for TC2, neglecting corrections due to heavy particles (Dirac fermions and extra vector-bosons) that are present in the top-triangle model, and focusing on the generic TC2 couplings. The top-triangle model-dependent corrections from the heavy states are of order a few percent, and their inclusion here or in our other computations would not change the results. The insensitivity of our analysis to model-dependent top-triangle effects is a confirmation that our results are generic for TC2 and other top-condensate models whose spectra have only  $H_t$  and  $\Pi_t$  particles present at low-energies in the top-mass generating sector of the theory.

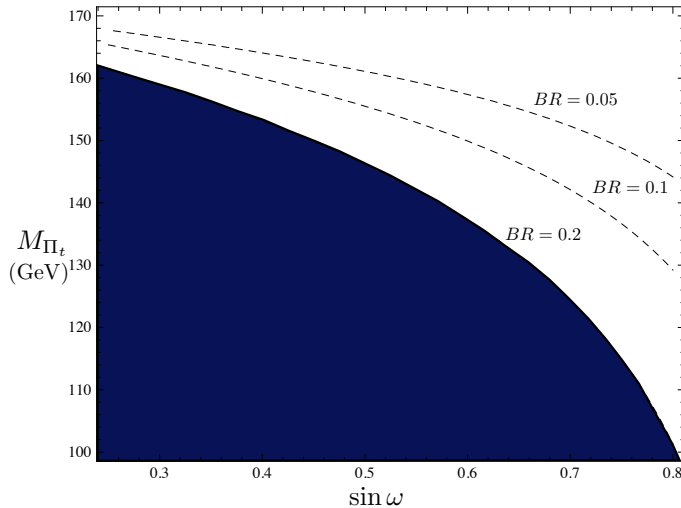


Fig. 1. Contours of constant branching ratio  $BR(t \rightarrow \Pi_t b)$ , as calculated from Eq. (8) in the  $(\sin \omega, M_{\Pi_t})$  plane, taking  $m_t = 172$  GeV and neglecting the bottom-quark mass. The dark blue region is excluded by Tevatron bound,<sup>32,33</sup> and  $M_{\Pi_t}$  must lie above the  $BR = 0.2$  line for the corresponding value of  $\sin \omega$ . The contours for  $BR = 0.1$  and  $0.05$  (dashed lines) are shown to indicate how this bound may evolve in the future if the bound continues to improve.

where we neglect the bottom-quark mass. From this we see that, for a given value of  $\sin \omega$ , there is a minimum value of  $M_{\Pi_t}$  such that  $BR(t \rightarrow \Pi^+ t) \lesssim 0.2$ . This lower bound on  $M_{\Pi_t}$  is illustrated in Fig. 1.

We may now return to the value of  $BR(H_t \rightarrow WW/ZZ)$ , which is crucial for understanding the LHC limits on these models. If kinematically allowed, the top-Higgs will decay predominantly to  $\Pi_t + W/Z$ ,  $2\Pi_t$ , or  $t\bar{t}$ .<sup>d</sup> The relevant couplings may be found in Ref. 23, where we ignore the small model-dependent corrections arising from heavy particles (see footnote c).

<sup>d</sup>In this analysis, we neglect off-shell decays since the three-point couplings for these processes are the same order of magnitude. Adding these processes would not change our results.

For decays to top-pion plus gauge boson,

$$\begin{aligned}\Gamma(H_t \rightarrow \Pi_t^\pm W^\mp) &= \frac{\cos^2 \omega}{8\pi v^2} M_{H_t}^3 \beta_V^3, \\ \Gamma(H_t \rightarrow \Pi_t^0 Z) &= \frac{\cos^2 \omega}{16\pi v^2} M_{H_t}^3 \beta_Z^3,\end{aligned}\quad (9)$$

where

$$\beta_V^2 \equiv \left[1 - \frac{(M_{\Pi_t} + M_V)^2}{M_{H_t}^2}\right] \left[1 - \frac{(M_{\Pi_t} - M_V)^2}{M_{H_t}^2}\right]. \quad (10)$$

For decays to two top-pions,

$$\Gamma(H_t \rightarrow \Pi_t^+ \Pi_t^-) = 2\Gamma(H_t \rightarrow \Pi_t^0 \Pi_t^0) = \frac{\lambda_{H\Pi\Pi}^2}{16\pi M_{H_t}} \sqrt{1 - \frac{4M_{\Pi_t}^2}{M_{H_t}^2}}, \quad (11)$$

where

$$\lambda_{H\Pi\Pi} = \frac{1}{2v \sin \omega} [(M_{H_t}^2 - 2M_{\Pi_t}^2) \cos 2\omega + M_{H_t}^2]. \quad (12)$$

And for decays to top-quark pairs,

$$\Gamma(H_t \rightarrow t\bar{t}) = \frac{3m_t^2}{8\pi v^2 \sin^2 \omega} M_{H_t} \left(1 - \frac{4m_t^2}{M_{H_t}^2}\right)^{3/2}. \quad (13)$$

By comparison, as we have previously discussed, the width to gauge-bosons is suppressed by  $\sin^2 \omega$

$$\begin{aligned}\Gamma(H_t \rightarrow W^+ W^-) &= \frac{M_{H_t}^3 \sin^2 \omega}{16\pi v^2} \sqrt{1 - x_W} \left[1 - x_W + \frac{3}{4} x_W^2\right], \\ \Gamma(H_t \rightarrow ZZ) &= \frac{M_{H_t}^3 \sin^2 \omega}{32\pi v^2} \sqrt{1 - x_Z} \left[1 - x_Z + \frac{3}{4} x_Z^2\right],\end{aligned}\quad (14)$$

where  $x_V = 4M_V^2/M_{H_t}^2$ .

If all decays are kinematically unsuppressed, and for the mass ranges we consider, a hierarchy of decay widths emerges:

$$\Gamma(H_t \rightarrow 2\Pi_t) \gtrsim \Gamma(H_t \rightarrow t\bar{t}), \quad \Gamma(H_t \rightarrow \Pi_t + W/Z) \gtrsim \Gamma(H_t \rightarrow WW/ZZ). \quad (15)$$

In particular, if kinematically allowed, the top-Higgs decays predominantly into pairs of top-quarks or top-pions. As we shall see, this implies that LHC searches are particularly sensitive to top-Higgs masses less than about 400 GeV. For this range of top-Higgs masses, LHC sensitivity depends crucially on the top-pion masses and whether the top-Higgs decays to either a top-pion pair or top-pion plus vector boson is allowed. LHC searches are most sensitive when these decay modes are suppressed and the  $BR(H_t \rightarrow WW/ZZ)$  is therefore as large as possible.



### 3. LHC Limits on the Top-Higgs

We are now ready to show how the recent ATLAS<sup>4</sup> and CMS<sup>5</sup> searches for the standard model Higgs boson lead to valuable LHC limits on the top-Higgs state. For the reasons described above, we consider top-Higgs masses ranging from 200 to 600 GeV. In this mass range, the standard model Higgs boson is produced primarily through gluon fusion and secondarily through vector-boson fusion.<sup>34</sup> The strongest limits<sup>4,5</sup> in this mass range come from searching for the Higgs boson decaying to  $W^+W^-$  or  $ZZ$ . In the narrow-width approximation for  $H_t$ ,<sup>e</sup> the inclusive cross section  $\sigma(pp \rightarrow H_t \rightarrow WW/ZZ)$  may be related to the corresponding standard model cross section through the expression

$$\begin{aligned} & \frac{\sigma(pp \rightarrow H_t \rightarrow WW/ZZ)}{\sigma(pp \rightarrow H_{SM} \rightarrow WW/ZZ)} \\ &= \frac{[\sigma_{gg}(pp \rightarrow H_t) + \sigma_{VBF}(pp \rightarrow H_t)] BR(H_t \rightarrow WW/ZZ)}{[\sigma_{gg}(pp \rightarrow H_{SM}) + \sigma_{VBF}(pp \rightarrow H_{SM})] BR(H_{SM} \rightarrow WW/ZZ)} \\ &\approx \frac{\left(\frac{1}{\sin^2 \omega} \sigma_{gg}(pp \rightarrow H_{SM}) + \sin^2 \omega \cdot \sigma_{VBF}(pp \rightarrow H_{SM})\right)}{\sigma_{gg}(pp \rightarrow H_{SM}) + \sigma_{VBF}(pp \rightarrow H_{SM})} \\ &\quad \cdot \frac{BR(H_t \rightarrow WW/ZZ)}{BR(H_{SM} \rightarrow WW/ZZ)}. \end{aligned} \tag{16}$$

While this relationship is appropriate for the ratio of inclusive cross sections, the experimental limits include detector-dependent effects such as acceptances and efficiencies. To the extent that gluon-fusion and vector-boson fusion Higgs (or top-Higgs) events differ, then this equation is only approximately correct. For Higgs masses between 200 and 600 GeV, however, the vector-boson fusion cross section accounts for only  $\mathcal{O}(10\%)$  of the standard model Higgs production cross-section, and we therefore expect the scaling relation will hold to better than this level of accuracy. We compute  $BR(H_t \rightarrow WW/ZZ)$  using Eqs. (9) - (14), and  $BR(H_{SM} \rightarrow WW/ZZ)$  using Eqs. (13) - (14) with  $\sin \omega \rightarrow 1$ , and we obtain the 7 TeV LHC standard model production cross sections  $\sigma_{gg,VBF}(pp \rightarrow H_{SM})$  from.<sup>34</sup> Putting this all together, we use Eq. (16) to convert the limits on the standard model Higgs in Refs. 4,5 into limits on the top-Higgs in TC2 models.

In Figs. 2 and 3 we show the ratio of  $\sigma(pp \rightarrow H_t \rightarrow WW/ZZ)$  divided by the corresponding quantity for the standard model Higgs, as a function

<sup>e</sup>We will justify the validity of this approximation for the regions in which the ATLAS and CMS bounds apply.

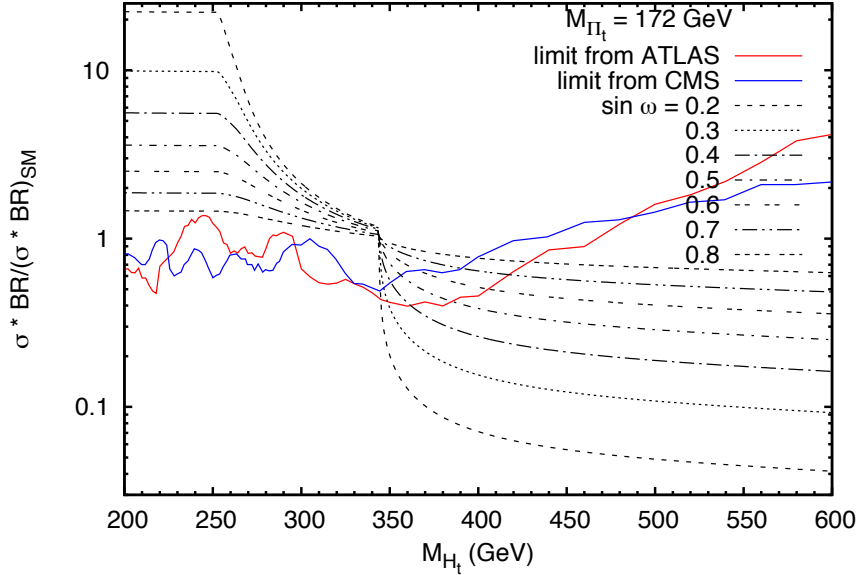


Fig. 2. LHC top-Higgs production cross section times  $WW$  branching ratio,  $\sigma(pp \rightarrow H_t \rightarrow WW)$ , relative to that of the standard model as a function of top-Higgs mass, for a top-pion mass  $M_{\Pi_t} = 172$  GeV and various values of  $\sin \omega = f_t/v$ . Also shown are the corresponding ATLAS<sup>4</sup> and CMS<sup>5</sup> 95% CL upper bounds on this ratio. Note the sharp drop in the branching ratio when  $t\bar{t}$  and  $2\Pi_t$  modes both open near 350 GeV. Regions excluded by this plot are shaded in medium red and orange hues in Fig. 5.

of  $M_{H_t}$  for various values of  $\sin \omega$ , and for  $M_{\Pi_t} = 172$  GeV and 400 GeV. Also plotted here are the recent 95% CL LHC upper bounds<sup>4,5</sup> on these quantities. For  $M_{\Pi_t} \simeq m_t = 172$  GeV, note the sharp drop in the branching ratio when the decay modes into  $t\bar{t}$  and  $2\Pi_t$  open near 350 GeV. Because of this drop in the branching ratio for vector boson pairs, the LHC limits on the top-Higgs are weaker when the top-pions are lighter. For  $M_{\Pi_t} = 400$  GeV, again the branching ratio falls sharply above 350 GeV as the  $t\bar{t}$  decay mode opens. Since  $BR(H_t \rightarrow WW/ZZ)$  is larger in the regions where  $M_{H_t} < M_{\Pi_t} + M_{W,Z}$ , the LHC limits on the top-Higgs are substantially stronger for heavier  $M_{\Pi_t}$ . The regions excluded by these plots in the  $(M_{H_t}, \sin \omega)$  plane are shaded in hues of red, orange, and gold in Fig. 5.

Earlier, in Fig. 1, we saw that the minimum  $M_{\Pi_t}$  that satisfies the Tevatron upper bound on  $BR(t \rightarrow \Pi^+ b)$ <sup>32,33</sup> depends on  $\sin \omega$ . Now, in Fig. 4 we plot the LHC top-Higgs production cross section times  $WW$  branching ratio,  $\sigma(pp \rightarrow H_t \rightarrow WW)$ , relative to that of the standard

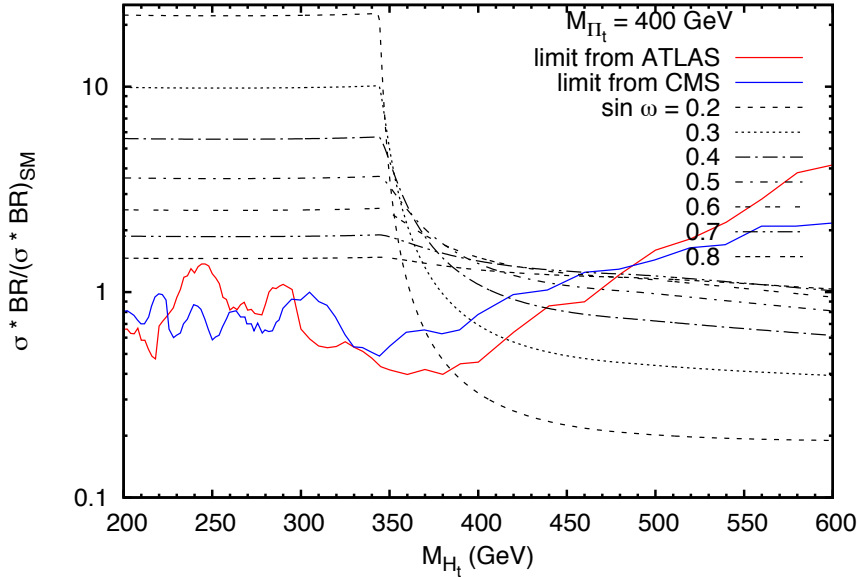


Fig. 3. As in Fig. 2, but for  $M_{\Pi_t} = 400$  GeV. The branching ratio drops at 350 GeV as the  $t\bar{t}$  decay mode opens. Regions excluded by this plot are shaded light gold in Fig. 5.

model as a function of top-Higgs mass, for combinations of  $\sin \omega$  and top-pion mass  $M_{\Pi_t}$  that saturate the Tevatron bound on  $BR(t \rightarrow \Pi^+ b)$ .<sup>32,33</sup> We also show the corresponding ATLAS<sup>4</sup> and CMS<sup>5</sup> 95% CL upper bounds on this ratio. Again, note the drop in the branching ratio when the  $\Pi_t W/Z$  mode opens. The regions excluded by this plot are shaded very dark blue in Fig. 5.

In translating the ATLAS and CMS limits on the standard model Higgs boson to the top-Higgs, we have used the narrow-width approximation. This breaks down for sufficiently large  $M_{H_t}$  and small  $\sin \omega$ . However, as we have seen, in the region where the ATLAS and CMS bounds apply to the top-Higgs, the decays to  $WW/ZZ$  dominate and those to  $\Pi_t W/Z$  or  $2\Pi_t$  are kinematically suppressed. For these parameter values the width of the top-Higgs is comparable to that of the standard model Higgs, and hence our scaling is valid.

Finally, Fig. 5 summarizes all of our results for bounds on the top-Higgs in models with strong top dynamics. The regions shaded very dark blue are completely excluded by the LHC searches for the standard model Higgs boson. We see that top-Higgs masses of 300 GeV or less are excluded at

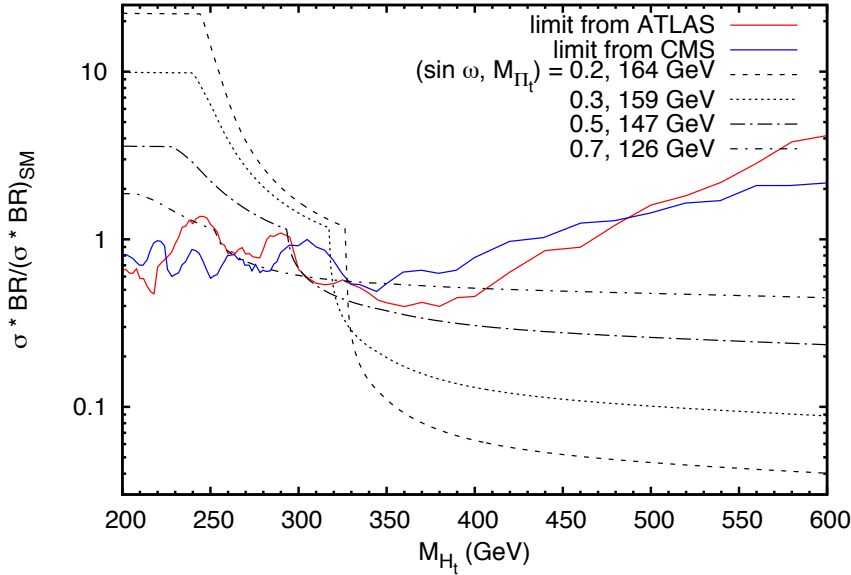


Fig. 4. Same plot as in Fig. 2, for combinations of  $\sin \omega$  and top-pion mass  $M_{\Pi_t}$  that saturate the Tevatron bound on  $BR(t \rightarrow \Pi b) \lesssim 0.2$ .<sup>32,33</sup> The regions excluded by this plot are shaded very dark blue in Fig. 5.

95% CL for any value of  $\sin \omega$  and for  $M_{\Pi_t} \gtrsim 150$  GeV. Moreover, when the top-pion is heavier than the top quark, all of the generic parameter range in TC2 models ( $0.25 \lesssim \sin \omega \lesssim 0.5$  and  $M_{H_t} \lesssim 2m_t$ ) is excluded at 95% CL.

#### 4. Discussion

This talk has shown that the LHC limits on the standard model Higgs boson<sup>4,5</sup> also constrain the top-Higgs state predicted in many models with new dynamics coupled strongly to top quark. Models of this kind include topcolor assisted technicolor, top seesaw, and certain Higgsless models. The top-Higgs state generically couples strongly to top-quarks, and is therefore produced through gluon fusion at an enhanced rate relative to the standard model Higgs boson. If the spectrum of the theory allows the branching ratio of the top-Higgs to vector boson pairs to be sufficiently high, which happens if the corresponding top-pion is sufficiently heavy, then current LHC searches for the standard model Higgs boson exclude the existence of the top-Higgs, as summarized in Fig. 5.

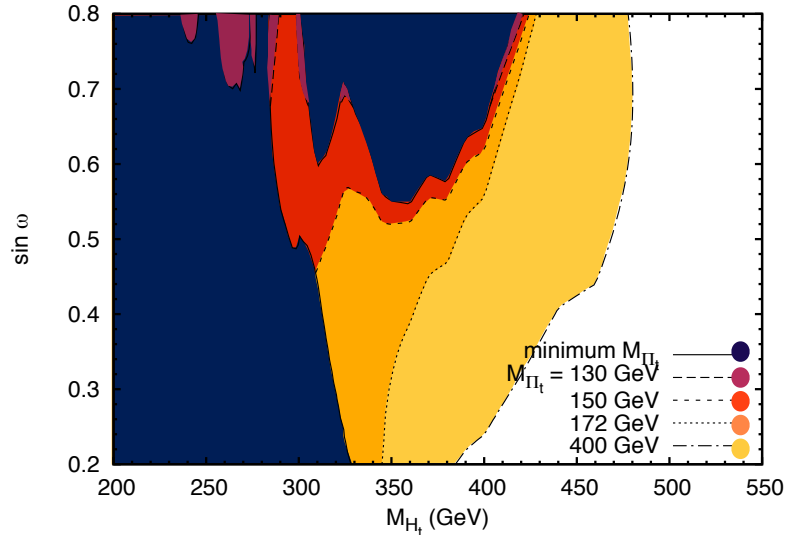


Fig. 5. Regions in the  $(M_{H_t}, \sin \omega)$  plane excluded by the ATLAS<sup>4</sup> and CMS<sup>5</sup> upper bounds on  $\sigma(pp \rightarrow H_t \rightarrow WW)$  for  $M_{\Pi_t} = 130$  GeV (dark wine regions outside long-dashed lines), 150 GeV (medium red regions above short-dashed line), 172 GeV (moderate orange region to left of dotted line) and 400 GeV (light gold region to left of dot-dashed line). Very dark blue regions are excluded for top-pion masses that saturate the Tevatron bound for a given value of  $\sin \omega$ .

Our results show that the relatively light top-Higgs states expected in generic TC2 models are tightly constrained. Moreover, as described in footnote c, we have used the effective theory supplied by the top triangle moose to confirm that these conclusions apply broadly to top-condensate models that have only  $H_t$  and  $\Pi_t$  particles in the low-energy spectrum of the sector responsible for generating the top quark mass.

In principle, models with top-Higgs masses larger than 350 GeV are still allowed. In this region, for small  $\sin \omega$ , the top-Higgs becomes a very broad state decaying predominantly into top-quark or top-pion pairs and LHC searches for this state may be difficult. Within the context of a TC2 model, however, it would be difficult to reach that region of parameter space. Theoretically, the non leading-log (or sub-leading in  $1/N$ ) corrections to the NJL approximation to the topcolor interactions could shift the top-

Higgs mass toward substantially larger values. However, precision flavor and electroweak analyses<sup>9</sup> prefer larger values of the cutoff  $\Lambda$  and make it unlikely that these effects are large enough to do so.

One avenue to constructing a viable dynamical theory with large  $M_{H_t}$  might be to pair technicolor with a “top-seesaw”<sup>35,36</sup> sector rather than a topcolor sector.<sup>39</sup> In a top-seesaw model, condensation of a heavy seesaw top-partner fermion breaks the electroweak symmetry, thereby severing the link between the top-quark mass and  $f_t$  illustrated by Eq. (2). Because of the increased value of  $f_t$ , a seesaw-assisted technicolor theory would feature both larger values of  $M_{H_t}$  and higher values of  $\sin \omega$  than are typical for TC2. In fact, just as the top-triangle moose serves as a low-energy effective theory for the top-Higgs and top-pion sectors of TC2 in the region of moose parameter space where  $f_t$  is relatively small, it may also be viewed as a low-energy effective theory for top-seesaw assisted technicolor when  $f_t$  is relatively large. In essence, a top-seesaw assisted technicolor theory smoothly interpolates between TC2 and the standard model with a heavy Higgs boson – a situation that is potentially allowed in the presence of weak isospin violation.<sup>37,38</sup>

As additional LHC data accumulates, we anticipate that further searches for signs of a Higgs decaying to vector boson pairs will either reveal the presence of a top-Higgs or significantly raise the lower bound on its mass. In either case, the implications for theories with new strong top dynamics will be profound.

### Acknowledgments

RSC and EHS were supported, in part, by the US National Science Foundation under grant PHY-0854889 and they are grateful to KMI for enabling their participation at this conference. BC and HEL were supported by the Natural Sciences and Engineering Research Council of Canada. AM is supported by Fermilab operated by Fermi Research Alliance, LLC under contract number DE-AC02-07CH11359 with the US Department of Energy.

### References

1. R. S. Chivukula, E. H. Simmons, B. Coleppa, H. E. Logan and A. Martin, arXiv:1108.4000 [hep-ph].
2. S. L. Glashow, Nucl. Phys. **22**, 579-588 (1961);  
S. Weinberg, Phys. Rev. Lett. **19**, 1264-1266 (1967);  
A. Salam, *Elementary Particle Theory, Nobel Symposium No. 8*, eds.: Svartholm, Almquist, and Wiksells, Stockholm, 1968;  
S. L. Glashow, J. Iliopoulos, L. Maiani, Phys. Rev. **D2**, 1285-1292 (1970).

3. P. W. Higgs, Phys. Lett. **12**, 132-133 (1964) and Phys. Rev. Lett. **13**, 508-509 (1964);  
F. Englert and R. Brout, Phys. Rev. Lett. **13**, 321-322 (1964);  
G. S. Guralnik, C. R. Hagen, T. W. B. Kibble, Phys. Rev. Lett. **13**, 585-587 (1964).
4. ATLAS Collaboration, "Update of the Combination of Higgs Boson Searches in 1.0 to 2.3 fb<sup>-1</sup> of pp Collisions Data Taken at  $\sqrt{s} = 7$  TeV with the ATLAS Experiment at the LHC," ATL-PHYS-PUB-2011-135, 22 August 2011.
5. CMS Collaboration, "Search for standard model Higgs boson in pp collisions at  $\sqrt{s} = 7$  TeV and integrated luminosity up to 1.7 fb<sup>-1</sup>," CMS PAS HIG-11-022, August 22, 2011.
6. C. T. Hill, Phys. Lett. B **345**, 483 (1995) [arXiv:hep-ph/9411426].
7. K. Lane and E. Eichten, Phys. Lett. B **352**: 382-387 (1995).
8. M. B. Popovic and E. H. Simmons, Phys. Rev. D **58**, 095007 (1998) [arXiv:hep-ph/9806287].
9. F. Braam, M. Flossdorf, R. S. Chivukula, S. Di Chiara and E. H. Simmons, Phys. Rev. **77**, 055005 (2008) [arXiv:0711.1127 [hep-ph]].
10. S. Weinberg, Phys. Rev. D **19**, 1277 (1979).
11. L. Susskind, Phys. Rev. **D20**, 2619-2625 (1979).
12. V. A. Miransky, M. Tanabashi and K. Yamawaki, Phys. Lett. B **221**, 177 (1989).
13. V. A. Miransky, M. Tanabashi and K. Yamawaki, Mod. Phys. Lett. A **4**, 1043 (1989).
14. Y. Nambu, Enrico Fermi Institute Preprint EFI-89-08.
15. W. J. Marciano, Phys. Rev. Lett. **62**, 2793 (1989).
16. W. A. Bardeen, C. T. Hill and M. Lindner, Phys. Rev. D **41**, 1647 (1990).
17. C. T. Hill, arXiv:hep-ph/9702320.
18. G. Buchalla, G. Burdman, C. T. Hill, D. Kominis, Phys. Rev. **D53**, 5185-5200 (1996). [hep-ph/9510376].
19. For a review of dynamical models of electroweak symmetry breaking, see C. T. Hill, E. H. Simmons, Phys. Rept. **381**, 235-402 (2003). [hep-ph/0203079].
20. R. S. Chivukula, Phys. Rev. Lett. **61**, 2657 (1988).
21. R. S. Chivukula, S. B. Selipsky, E. H. Simmons, Phys. Rev. Lett. **69**, 575-577 (1992). [hep-ph/9204214].
22. R. Sekhar Chivukula, N. D. Christensen, B. Coleppa and E. H. Simmons, Phys. Rev. D **80**, 035011 (2009) [arXiv:0906.5567 [hep-ph]].
23. R. S. Chivukula, E. H. Simmons, B. Coleppa, H. E. Logan, A. Martin, Phys. Rev. **D83**, 055013 (2011). [arXiv:1101.6023 [hep-ph]].
24. R. S. Chivukula, A. G. Cohen and K. D. Lane, Nucl. Phys. B **343**, 554 (1990).
25. Y. Nambu, G. Jona-Lasinio, Phys. Rev. **122**, 345-358 (1961).
26. G. 't Hooft, Nucl. Phys. **B72**, 461 (1974).
27. H. Pagels, S. Stokar, Phys. Rev. **D20**, 2947 (1979).
28. S. Dimopoulos, L. Susskind, Nucl. Phys. **B155**, 237-252 (1979).
29. E. Eichten, K. D. Lane, Phys. Lett. **B90**, 125-130 (1980).
30. C. T. Hill, C. N. Leung, S. Rao, Nucl. Phys. **B262**, 517 (1985).

31. H. M. Georgi, S. L. Glashow, M. E. Machacek, D. V. Nanopoulos, *Phys. Rev. Lett.* **40**, 692 (1978).
32. T. Aaltonen *et al.* [CDF Collaboration], *Phys. Rev. Lett.* **103**, 101803 (2009) [arXiv:0907.1269 [hep-ex]].
33. V. M. Abazov *et al.* [D0 Collaboration], *Phys. Lett. B* **682**, 278 (2009) [arXiv:0908.1811 [hep-ex]].
34. LHC Higgs Cross Section Working Group, updated May 25, 2011, <https://twiki.cern.ch/twiki/bin/view/LHCPhysics/CERNYellowReportPageAt7TeV>.
35. B. A. Dobrescu and C. T. Hill, *Phys. Rev. Lett.* **81**, 2634 (1998) [arXiv:hep-ph/9712319].
36. R. S. Chivukula, B. A. Dobrescu, H. Georgi and C. T. Hill, *Phys. Rev. D* **59**, 075003 (1999) [arXiv:hep-ph/9809470].
37. R. S. Chivukula, C. Hoelbling and N. J. Evans, *Phys. Rev. Lett.* **85**, 511 (2000) [arXiv:hep-ph/0002022].
38. H. J. He, C. T. Hill and T. M. P. Tait, *Phys. Rev. D* **65**, 055006 (2002) [arXiv:hep-ph/0108041].
39. For steps in this direction, see H. S. Fukano, K. Tuominen, [arXiv:1102.1254 [hep-ph]].